

CHAPTER II

THEORY AND LITERATURE REVIEWS

THEORY

2.1 Optoelectronic applications

Optoelectronics is an interesting branch of electronics that combines both electronics and optics together thus optoelectronic devices can interconvert between light and electricity in their operations. In photoconductive devices i.e. photo resistors, photodiode and phototransistor etc. can activate or deactivate electric circuits by the detection in the light intensities. On the other side, Photovoltaic devices, such as solar cell, optical sensor, produce a voltage when these are exposed to light that corresponding to a potential difference between p-n junctions depended on the light intensity [23].

As a novel emerging science with great applications, organic optoelectronic materials with special functionalities stem increasing ability to manipulate and tune the properties of organic and polymeric materials by the structural modification [23]. Organic optoelectronic devices, i.e. organic electroluminescent device (OLECD), organic photovoltaic (OPV) and organic thin film transistors (OTFT), have attracted significant attention in both academic and industries due to their lower cost compared to inorganic-based devices and great application potential in flat-panel and flexible display [24].

The electronic structure of all organic semiconductors is based on conjugation π -electrons. A conjugated organic system is made of an alternation between single and double carbon-carbon bonds. Single bonds are known as σ -bonds and are associated with localized electron, and double bonds contain a σ -bond and a π -bond. The π -electrons can jump from site to site between carbon atoms, overlap of π -orbitals along the conjugation path, which causes the wave functions to delocalize over the conjugated backbone. The π -orbital are either empty (lowest unoccupied molecular orbital-LUMO) or filled with electrons (highest occupied molecular orbital-HOMO). The difference of energy level between HOMO and LUMO is called energy gap (E_{gap}). It causes difference in photophysical and electrochemical properties in such organic molecules [25].

Conjugated polymers and molecules have the immense advantage of facile, chemical tailoring to alter their properties, such as the energy gap. Conjugated polymers combine the electronic properties known from the traditional semiconductors and conductors with the ease of processing and mechanical flexibility of plastics. Therefore, this new class of materials has attracted considerable attention owing to its potential of providing environmentally safe, flexible, lightweight, inexpensive electronics. The cost reduction mainly results from the ease of processing from solution. While the solution processing requires soluble polymers, poly[*p*-phenylene vinylene] (PPV, **Chart 2-1**) is hardly soluble and therefore not a very suitable material. Attachment of side-groups to the conjugated backbone, as in poly[2-methoxy-5-(3',7'-dimethyloctyloxy)-1,4-phenylene vinylene] (MDMO-PPV, **Chart 2-1**), enhances the solubility of the polymer enormously. Furthermore, the nanoscale morphology, affecting the optoelectronic properties of these polymer films, can be controlled by proper choice of the position and nature of these side groups. The development of regio-regular polythiophenes, such as region-regular poly[3-hexylthiophene] (P3HT, **Chart 2-1**) showed the huge effect side-groups can have on charge-carrier mobility [25].

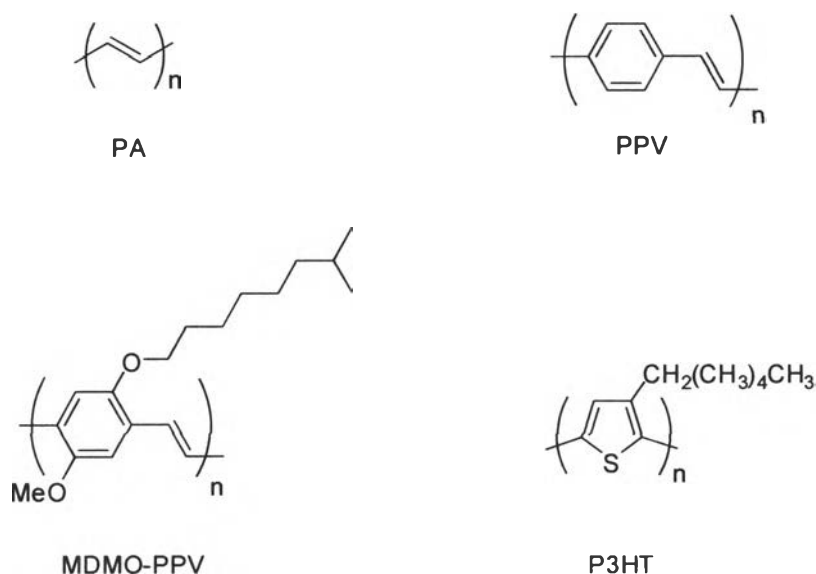


Chart 2-1: Molecular structures of trans-polyacetylene (PA), poly(*p*-phenylenevinylene) (PPV), a poly[2-methoxy-5-(3',7'-dimethyloctyloxy)-1,4-phenylene vinylene] (MDMO-PPV), and a poly[3-hexylthiophene] (P3HT).

Conjugated polymers have been extensively studied for their potential applications in light emitting diodes, organic lasers, thin film transistors, and solar cells [26-28]. Among them, polyacetylene (PA, **Chart 2-1**) with alternating single and double bonds is the best-known conjugated polymer because polyacetylene possesses metallic conductivity upon doping. This has opened up new research opportunities in the field of electro active macromolecules [29, 30]. The incorporation of functional pendants into the polyacetylene structure not only overcomes its disadvantages of intractability and instability, but also endows new functional properties such as photo- and electroluminescence [31], optical activity (chirality) [32], liquid crystallinity [33], and nonlinear optics (NLO) [34]. In 2014, Bin L. et al. synthesized a group of novel polyacetylenes containing BODIPY pendants using a $[\text{Rh}(\text{nbd})\text{Cl}]_2\text{-Et}_3\text{N}$ catalyst (**Chart 2-2**) [35]. The pendant BODIPY unit has been directly conjugated to the polyacetylene backbone either through the 8 position of the BODIPY cores in **P1** or through the 3 position in **P2** and **P3**. Interestingly, the spectroscopy results showed that little electronic interaction existed between the BODIPY chromophoric units and the polyacetylene main chain for **P1**. However, the electronic interaction between the side pendant and the main chain became notable for **P2** and **P3**, resulting in a significant broadening and red-shift of their UV-vis absorption and fluorescence emission wavelengths in comparison with those of their respective monomers. The polymers displayed thermal stabilities and nonlinear optical properties that were dependent on the connectivities of the BODIPY pendants and the polyacetylene backbones. **P1** exhibits relatively better thermal stability and poorer nonlinear optical properties than **P2** and **P3**.

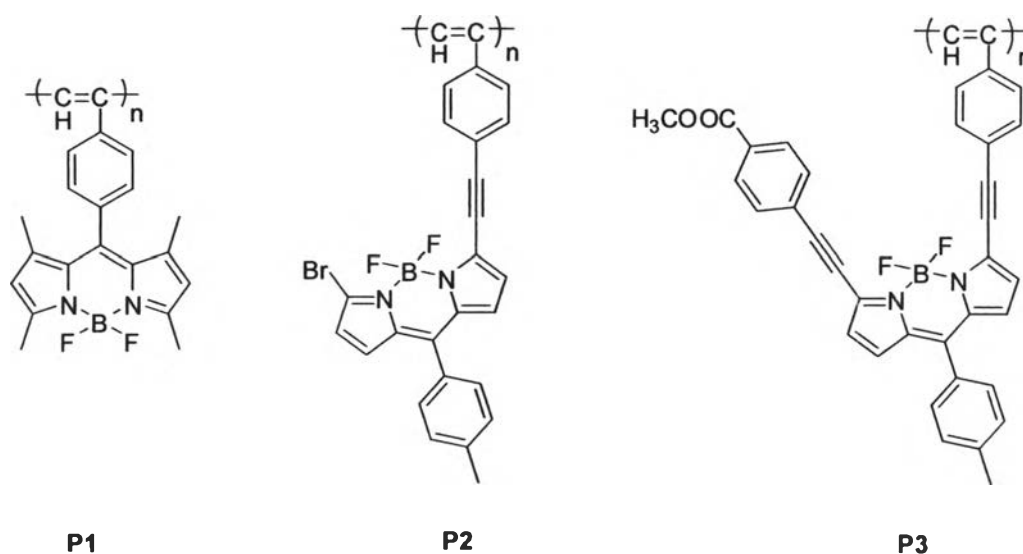


Chart 2-2: Polyacetylenes containing BODIPY pendants reported by Bin L. et al.

As regards the main process of photovoltaic energy conversion by bulk-heterojunction solar cell (**Figure 2-1**), the p-type and n-type materials must have a good balance of the electronic levels [36]. Theoretically, the LUMO of the donor must have energy higher than the LUMO of acceptor, and the HOMO of the acceptor must also have a lower energy of the HOMO of donor. The foremost process is light absorption by active layer, resulting in electrons in donor phase excited from the HOMO to the LUMO. Then, the separated electrons from exciton transfer to the LUMO energy level of acceptor phase and diffuse to cathode. Finally, the electron transfers complete the electric circuit, leading to the electricity.

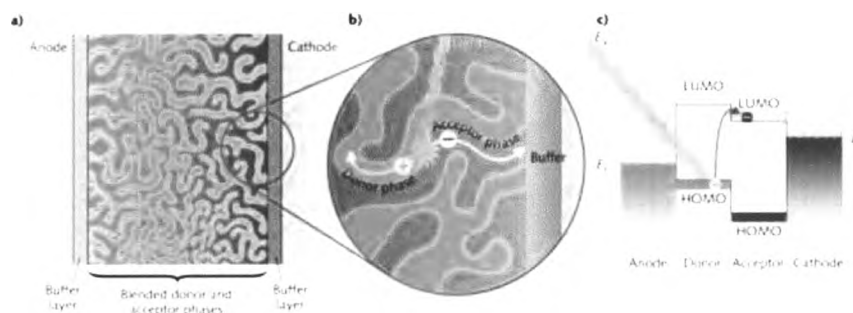


Figure 2-1: a) In a bulk-heterojunction organic photovoltaic design, b) light absorption generates electrons and holes that travel through the donor and acceptor phases, c) the energy level diagram [37]

The one of the most popular p-type organic materials are poly(p-phenylene vinylene) (PPV) and poly(3-hexylthiophene-2,5-diyl) (P3HT), which have a low energy gap with high mobility of the positive charges [38]. The most widely used n-type organic materials is a fullerene derivative, [6,6]-phenyl C₆₁-butyric acid methyl ester (PCBM), which has better solubility in several common organic solvents compared to fullerene C₆₀ (Figure 2-2).

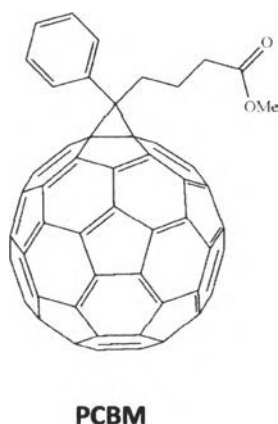


Figure 2-2: Chemical structure of [6,6]-phenyl C₆₁-butyric acid methyl ester (PCBM)

2.2 Molecular design of organic photosensitizers

For organic optoelectronic devices, the molecular design of the organic photosensitizer comes to an important section for improving the device efficiency. Depending on types of the optoelectronic devices the organic photosensitizer should have all of the following properties:

- (i) Suitable physical properties for example solubility, high thermal stability, long-term stability in working environment,
- (ii) Favorable photophysical properties such as wide absorption band and high extinction coefficient for solar cell, and
- (iii) Desirable electrochemical properties e.g. appropriate redox potentials [39].

2.3 Jablonski energy diagram of organic molecule

Electronic transitions can be occurred between the ground states and excited states energy levels. The several energy gap levels involved in the absorption and emission of light by a chromophore are normally presented by Jablonski energy diagram [40] (Figure 2-3).

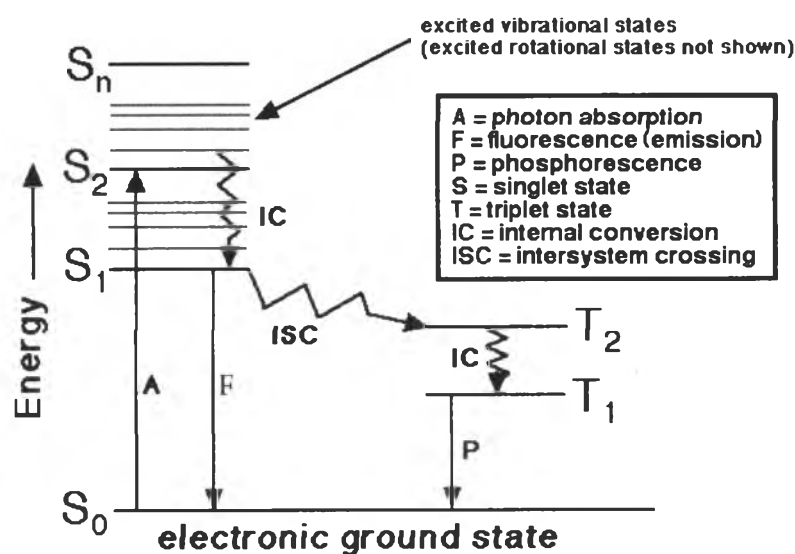


Figure 2-3: Simplified Jablonski diagram

The Jablonski diagram demonstrates a singlet ground state (S_0) and excited singlet states ($S_2, S_3 \dots$) in horizontal lines. Different triplet states are represented by T_1, T_2 . The thicker lines denote electronic energy levels, while the thinner lines denote the various vibrational energy states. Straight arrows show electronic transitions associated with absorption or emission of photons. Curl arrows show a molecular internal conversion or non-radiative relaxation processes [41]

The first transition is the absorbance of the photons by the molecule. Normally, the molecular absorption of the photons at a specific wavelength causes electronic excitation from the ground state to some vibrational level in the excited singlet state. If the absorbed photon has higher energy than of necessary for a simple electronic transition, the excess energy is usually converted into vibrational or rotational energy. The broadening of absorption spectrum is resulted from the closely spaced of vibrational energy levels plus thermal motion that enable a range of the photon energy to match a particular transition. After that, several processes

will occur with various probabilities, but the most likely to happen would be a relaxation to the lowest vibrational energy level of the first excited state (S_1). This process is known as internal conversion or vibrational relaxation. An excited molecule exists in the lowest excited singlet state for periods before finally relaxing to the ground state (S_1 to S_0). If relaxation from this long-lived state is accompanied by the emission of a photon, the process is normally known as fluorescence. It is the reason why the fluorescence spectrum is always shifted to higher wavelength compared to the corresponding absorption spectrum. This shift is called Stokes shift. If the phenomenon known as intersystem crossing occurred instead of a normal emission, the spin multiplicity of excited molecule will change from singlet to triplet state. This event is relatively rare, but eventually results in emission of photon through phosphorescence (T_1 to S_0). Transitions from the triplet excited state to the singlet ground state are forbidden, resulting in rate constants for triplet emission is slower than those of fluorescence [42].

2.4 4,4-Difluoro-4-bora-3a,4a-diaza-s-indacene (BODIPY)

2.4.1 Fundamental properties

Much attention has been devoted to the chemistry of 4,4-difluoro-4-bora-3a,4a-diaza-s-indacene (BODIPY). The IUPAC numbering system for BODIPY dyes is different to that used for dipyrromethene and dipyrromethane [43], and this can lead to confusion. However, the terms α -, β -positions, and *meso*- are used in just the same way for both systems (Chart 2-3).

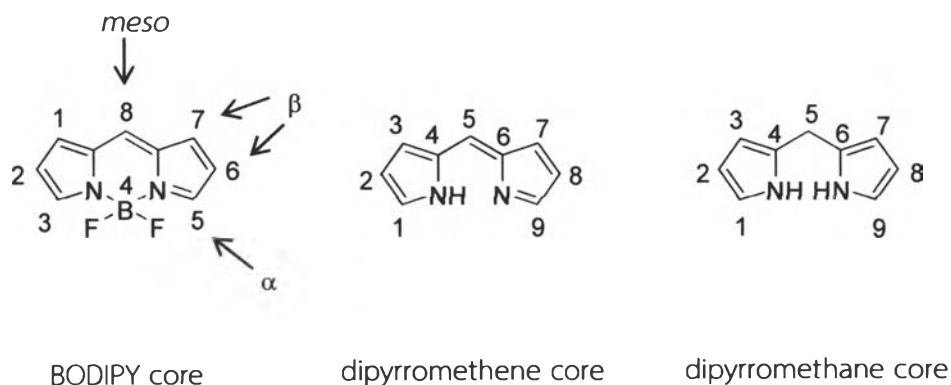


Chart 2-3: Numbering systems in BODIPY, dipyrromethene and dipyrromethane cores

BODIPY core has a zwitterionic structure where a positive charge is delocalized throughout the π -system. It was first proposed that the boron atom has a net positive charge due to the electronegative nature of both the fluorine and nitrogen atoms linked to it. However quantum mechanical calculations have shown the negative electronic density of the molecule localized mainly on the F atoms and to a lesser extent the N atoms. The resonance structures are shown in **Figure 2-3**. The BF_2 group does not take part in the delocalized π -system but instead gives rigidity to the structure. Thus BODIPYs can be classified as quasi-aromatic molecules [44].

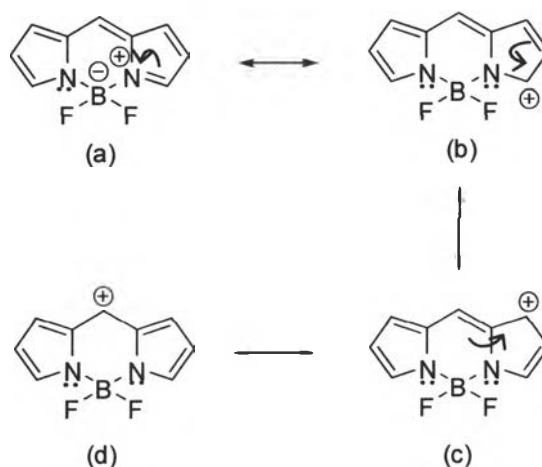


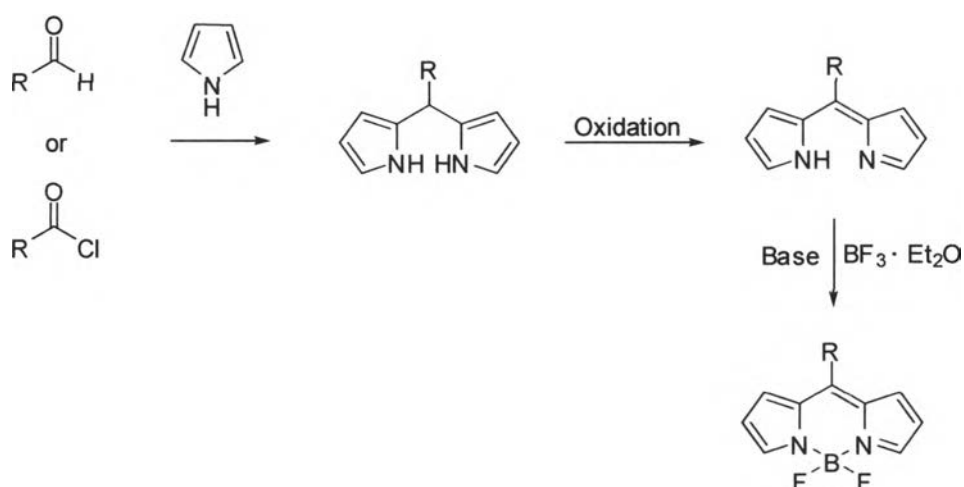
Figure 2-4: Zwitterionic structures of BODIPYs

BODIPY dye consists of a dipyrromethene ligand complexed with a disubstituted boron atom. BODIPY are among the most recent investigated fluorescence dyes for a variety of analytical and imaging applications [5, 6]. Due to their favorable photophysical and optoelectronic properties that include high photostability, high extinction coefficient and high fluorescence quantum yields. BODIPYs have attracted special interest in drug discovery [45], biomedical imaging [46] and optical sensing [10, 47].

2.4.2 Synthesis of BODIPY

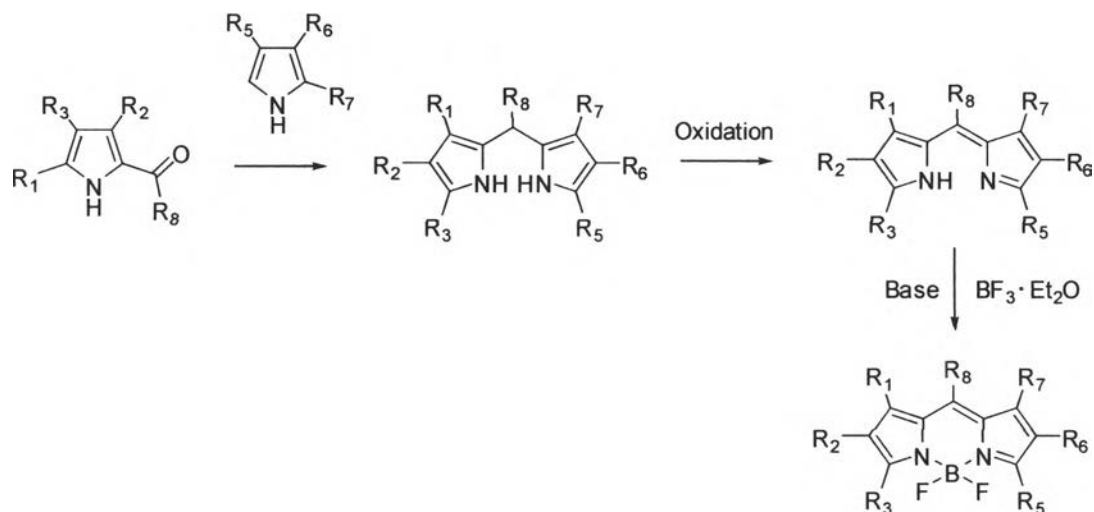
2.4.2.1 Basic procedure

Construction of the dipyrromethene precursor is based on the well-known pyrrole condensation reaction. A highly electrophilic carbonyl compound is used to form the methane bridge between two pyrrole units. The BODIPY dyes are obtained after oxidation with DDQ and subsequent complexation with boron, as shown in **Scheme 2-1** for symmetric BODIPY dyes [48].



Scheme 2-1: General synthetic pathway of symmetric BODIPY dyes

Asymmetric BODIPY dyes are usually obtained by condensation of a carbonyl-containing pyrrole with another pyrrole molecule that is not substituted at the 2-position [48]. BODIPY-based biological labels [49, 50] are prepared by this particular method (**Scheme 2-2**).



Scheme 2-2: General synthetic pathway of asymmetric BODIPY dyes

2.4.2.2 Structural modification of BODIPY

The main objective of the structural modification of BODIPY are listed below:

- To tune photophysical properties such as absorption, emission wavelength, molecular extinction coefficients of absorption and fluorescence quantum yield.
- To obtain the desirable physical properties e.g. solubility, chemical, thermal stability and electrical stability.
- To achieve the appropriate molecular orientation in the film.
- To tune electrochemical properties such as redox potentials.

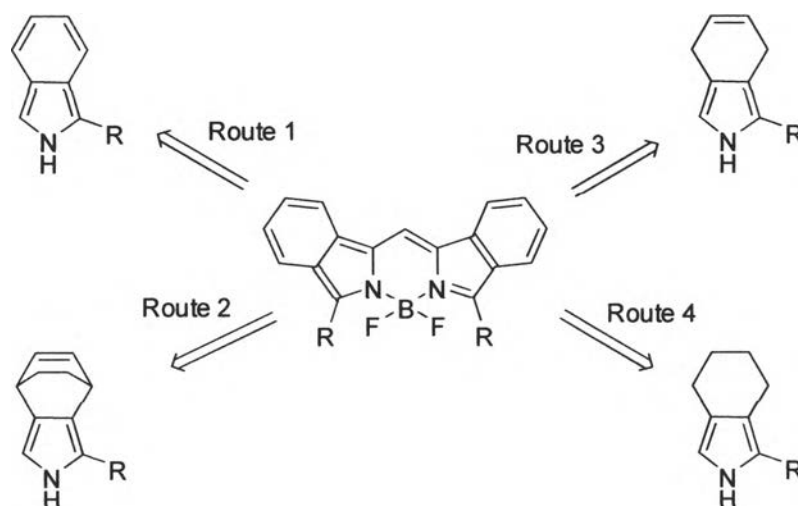
2.5 Extension of pi-electron conjugation of BODIPYs

2.5.1 Overview

Obtaining BODIPY dyes exhibiting absorption and emission in the NIR regions of the spectrum requires the presence of an extended delocalization pathway. Absorption in near IR region of spectrum is generally useful for biomedical applications such as photodynamic therapy (PDT) [51], *in vivo* optical imaging and sensing [13]. Several strategies are proposed to achieve this type of BODIPY dye.

The most direct method is to use pyrrole precursors bearing phenyl, vinyl, or thienyl group at the α -position [6, 52].

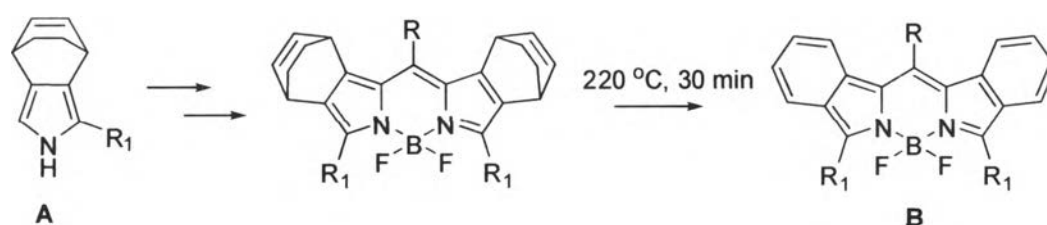
Another approach is the use of benzo-fused pyrrole, prepared from closely related pyrrolic precursors to isoindole. Some synthetic routes to BODIPYs are depicted in **Scheme 2-3** [53]. Since, the most straightforward method of acid-catalyzed condensation of aromatic aldehyde with 2H-isoindole (Route 1) is not possible due to the high reactivity, instability of the pyrrole precursor and other pyrrolic derivatives have to be employed. Another approach utilizing bicyclooctadiene-fused pyrrole (Route 2) represents the classical Ono, N. et al. method [54], but however suffers from certain drawbacks, as discussed before i.e. low overall yields and limit to special substrates. Alternatively, the benzo-BODIPY system can be assembled by the use of stable pyrrolic compounds such as 4,7-dihydroisoindole and 4,5,6,7-tetrahydroisoindole (Route 3 and 4), described by Filatov, M.A. et al. [53] and Borek, C. et al. [55] respectively, where the final aromatization step can be performed by oxidative dehydrogenation with DDQ. These approaches, so far, have not been developed into a general method of BODIPY synthesis, despite the preparation of π -extended dipyrins from 4,7-dihydroisoindole as recently reported by Filatov, M.A. and co-workers [56].



Scheme 2-3: Synthetic routes of benzo-BODIPYs

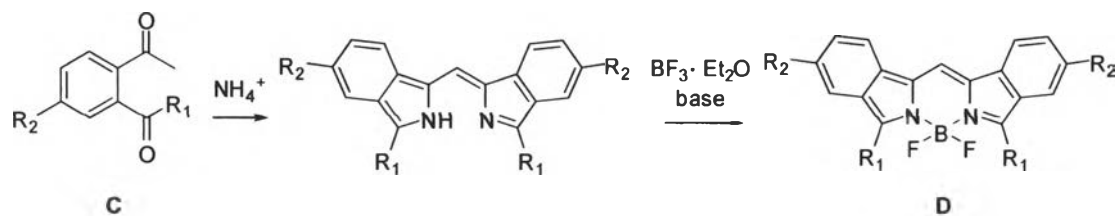
2.5.2 Benzo-BODIPY synthesis

Currently, the synthetic approaches to the meso-substituted benzo-BODIPY **B** (Scheme 2-4) includes the Ono, N. et al. method [56], which is based on the strategy of benzoporphyrins synthesis and centers around the masked isoindoles i.e. bicyclo octadiene-fused isoindole **A**. Such pyrroles fused with non-aromatic rings are readily available from Barton-Zard isocyanoacetate chemistry and appear to be useful synthesis for other π -extended pyrrole-based macrocycles [57]. In this approach, the precursor isoindole **A**, is condensed with aromatic aldehyde under typical Lindsey conditions, followed by the treatment with *N*-ethyl-*N*, *N*-diisopropyl amine and $\text{BF}_3 \cdot \text{OEt}_2$ to generate the bicycle octadiene-fused BODIPY system. Subsequently, the meso-substituted benzo-BODIPY **B** is generated by the retro Diels-Alder reaction upon heating the masked BODIPY system to 220 °C under reduced pressure (30 mmHg) for 30 minutes. Though this approach enables the fast expansion of the scope and preparative value of the benzo-BODIPYs, the major drawback of this methodology includes the severe reaction conditions required for the final aromatization step to effect the ethylene extrusion, which often leads to considerable loss of the product at final stage of the long synthesis [58].



Scheme 2-4: Synthesis of benzo-BODIPY **B** from isoindole **A**

The *meso*-unsubstituted benzo-BODIPY **D**, initially developed by Haugland, R.P. [57] utilizes the substituted 2-acylacetophenones **C** (Scheme 2-5) as the building units to benzo-BODIPY derivatives [59, 60]. Compound **C** is first condensed with ammonia to generate the dibenzo-fused dipyrin, which after treatment with Hunig's base and BF_2 -chelation, affords the constrained benzo-BODIPY dyes in good overall yields. This synthetic methodology is unique as it allows the introduction of various functional groups at the 5-position on the isoindole ring for further derivatization of the BODIPY dyes.



Scheme 2-5: Synthesis of benzo-BODIPY **D** from 2-acylacetophenone **C**

2.6 Thiophene

Thiophene is a heterocyclic five-membered compound with the formula C_4H_4S (**Chart 2-4**). Its aromaticity was indicated by its extensive substitution reactions. Thiophene and its derivatives are found in petroleum. The thiophenic content of oil and coal is separated via the hydrodesulfurization process. Thiophene has a structure analogous to pyrrole and due to π -conjugation system, it perform as a higher reactive benzene derivatives [61].

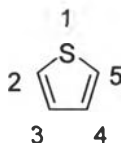


Chart 2-4: Structure of thiophene

Thiophene derivatives have been found to exhibit a wide range of biological activities [18] and medicinal usefulness as chemotherapeutics, while many of them have also been used in various materials science applications [19]. Oligothiophenes are often utilized as building blocks in the preparation of organic materials for use as organic semiconductors [20] because of their excellent electronic properties and other features such as chemical resistance, relative ease of synthesis and processability. As a consequence, there are many classes of oligothiophenes that serve in applications such as organic light-emitting diodes (LEDs) [62], organic field-effect transistors [63], photovoltaics [64], nonlinear optics [65], biology [66], and optically pumped lasers [67]. Based on a thorough understanding of structure-property relationships and the ingenuity of synthetic chemists, ambipolarity, tenability, high quantum efficiencies, and physical stability have all been achieved [68]. The thiophenes are among the most promising units for use to connect chromophoric centers and to provide interesting optical properties. Furthermore, the high polarizability of sulfur atoms in thiophene rings leads to a stabilization of the

conjugated chain and to excellent charge transfer properties, which make them as promising candidates for organic electronic devices. [69, 70].

LITERATURE REVIEWS

(1) In 2011, D. Collado, *et al.* synthesized several new push-pull oligothiophenes based on the electron accepting BODIPY and the well-known oligothiophenes substituted with *N,N*-dialkylamino group to enhance their electron-donor ability (**Chart 2-5**) [71]. A complete characterization of their photophysical, electrochemical, and vibrational properties was carried out. From the point of view of material applications, these systems can be used for solar cell applications due to both the good visible and NIR absorbing characteristics and ambipolar redox behavior, which is a key requirement for attaining high yields of charge-separated states after light absorption. Rousseau, T. *et al.* have published the photovoltaic properties of a heterojunction solar cell based on a BODIPY oligothiophene dyes. It displayed up to 2.20% conversion efficiency [72].

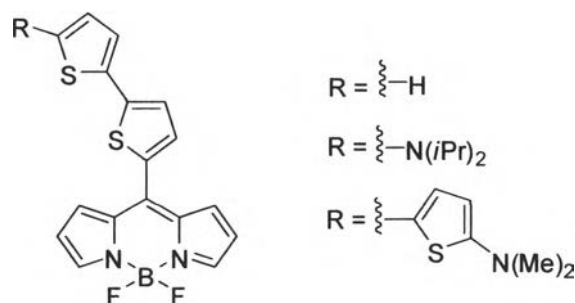
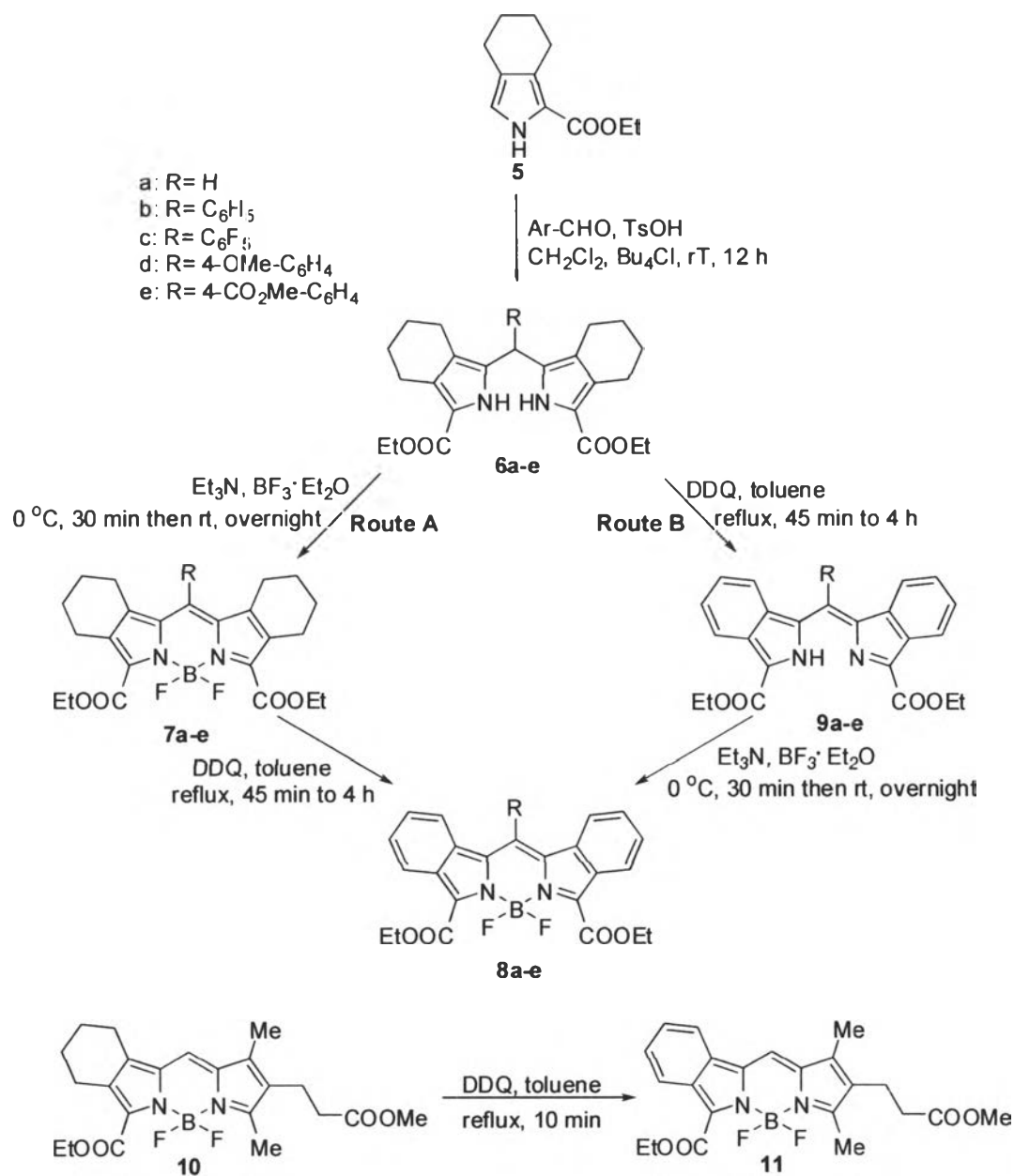


Chart 2-5: BODIPY-bithienyl derivatives reported by D. Collado, *et al.*

(2) In 2012, T. Uppal, *et al.* reported a series of new functional benzo-BODIPY dyes [13], synthesized from a common tetrahydroisoindole precursor following two different synthetic routes (**Scheme 2-6**). The benzo-BODIPY show strong red-shifted absorptions and emissions, about 50–60 nm per benzoannulated ring, with the maximum wavelength of 589–658 and 596–680 nm, respectively. In particular, benzo-BODIPY **8c** bearing a *meso*-C₆F₅ group showed the highest absorption and emission maxima, along with the lowest fluorescence quantum yield (0.31 in CH₂Cl₂), on the other hand benzo-BODIPY **11** showed the highest quantum yield (0.99) in this series. Cellular investigations using human carcinoma HEp2 cells revealed high

plasma membrane permeability for all benzo-BODIPYs, low dark and phototoxicities and intracellular localization in the cell endoplasmic reticulum, in addition to other organelles. This study indicates that benzo-BODIPY, in particular the highly stable *meso*-substituted BODIPY, is promising fluorophores for bioimaging applications.



Scheme 2-6: Synthesis of benzo-BODIPYs described by T. Upoal, et al.

(3) In 2012, K. Tikhomirova, *et al.* synthesized a series of 2,3,7,8-biscyclohexano-fused diethyl 5-aryldipyrin-1,9-dicarboxylates (**12**) (**Figure 2-4**) [73]. The obtained compounds were shown to exist in two equilibrium forms in solution, with one exhibiting a visible absorption band ($\lambda_{\text{abs}} = 468\text{--}485\text{ nm}$) and the other vis-silent form having no absorption band in the visible region. The vis-silent form has been isolated and characterized by NMR analysis. Quantum chemical calculations were also performed and confirmed the spectroscopic findings. These two different forms were also characterized as their Mg_2^+ complexes and investigated by UV/Vis and by NMR spectroscopic analyses, where the clear difference was noted.

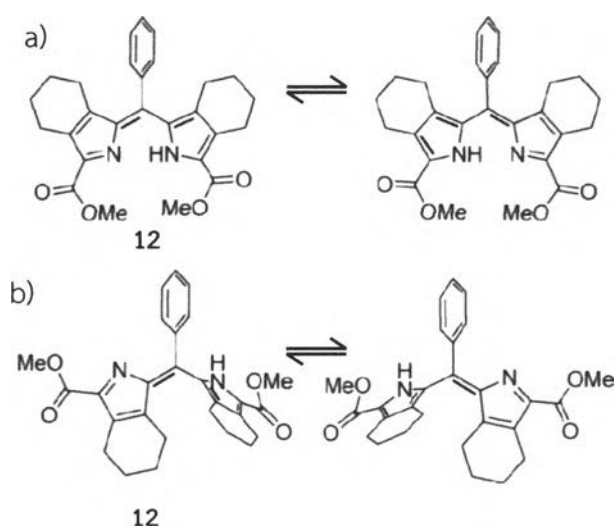


Figure 2-5: A corresponding schematic representation of their degenerate spatial reorganization in (a) visible form and (b) visible-silent form